https://doi.org/10.5194/egusphere-2025-3909
Preprint. Discussion started: 3 September 2025

Compound droughts have become more widespread globally

Marko Kallio[1,*#], Pihla Seppälä[1,2,*], Lauri Ahopelto[2], Amy Fallon[1,3], Pekka Kinnunen[4], Matias Heino[1], and Matti Kummu[1,#]

1 Water and development research group, Aalto University, Espoo, Finland
2 Finnish Environment Institute (Syke), Helsinki, Finland
3 Gulbali Institute, Charles Sturt University, New South Wales, Australia
4 Pellervo Economic Research PTT, Helsinki, Finland

* *Contributed equally to the work*

\# *Corresponding authors*: Marko Kallio (marko.k.kallio@aalto.fi) and Matti Kummu (matti.kummu@aalto.fi)

Abstract.

Compound droughts, in which meteorological, hydrological, and agricultural drought occur simultaneously, have a more substantial impact on ecological and socio-economic systems than any drought type alone. Yet, the global patterns – and particularly the multi-decadal trends – of these co-occurring droughts remain poorly understood. We analyse the global co-occurrence of meteorological, agricultural, and hydrological droughts from 1961 to 2020 using run theory and empirical drought indices from three global hydrological models (GHMs), each forced with three different meteorological forcing datasets. Our results indicate that compound droughts and their characteristics show distinct spatial patterns, varying across different hydrological regions. The findings suggest that compound droughts have become more widespread globally, particularly in the hydrological regions (i.e., hydrobelts) near the equator and in the southernmost regions, where the number of days under compound drought has increased rapidly over the past 60 years. Our results also show that compound drought behaviour in the boreal hydrobelt significantly differs from all other hydrobelts, showing a general wetting trend and no increase in compound droughts. We also, however, find a high uncertainty in the ensemble, highlighting a need to global hydrological modelling aimed toward droughts specifically. The results provide valuable global insights into complex phenomena of compound droughts, helping in drought preparedness actions and planning.

1 Introduction

Droughts, as one of the costliest natural hazards, have threatened economic growth and caused significant environmental and agricultural damage throughout human history (Vicente-Serrano et al., 2010; Wu et al., 2022). Droughts commonly originate from the lack of precipitation and can propagate through the hydrological cycle, developing into various different drought types involving e.g. precipitation, soil moisture and runoff, discharge or groundwater levels (Mishra and Singh, 2010; Wilhite

https://doi.org/10.5194/egusphere-2025-3909
Preprint. Discussion started: 3 September 2025

and Glantz, 1985). The effects of drought on ecology and human societies depend on the part of the hydrological cycle they affect, and may impact, for instance, agriculture, transportation, power generation, commerce and industry, ecosystems and water quality (Van Loon, 2015). The temporal and spatial co-occurrence of these different drought types is referred to as 'compound drought'. The impacts of compound droughts on ecosystems and socio-economic sectors are more significant and serious than those of individually occurring drought types (Wu et al., 2022; Zscheischler et al., 2020). As it is anticipated that drought hazards will become more frequent and severe in many regions of the world due to climate change (e.g. Spinoni et al., 2020; Wang et al., 2021), it is important to understand the dynamics of compound droughts globally, particularly because of the inherent uncertainty in the estimates of drought trends over the past century due to a lack of direct observations and dependence on the chosen drought index (Alahacoon and and Edirisinghe, 2022; Mukherjee et al., 2018).

Climatic and physiographic differences between regions of the globe lead to distinct hydrological processes across landscapes (Beck et al., 2018; Linke et al., 2019; Meybeck et al., 2013). Most existing research about compound drought occurrence, however, is on smaller case study areas (e.g. Feng et al., 2023; Li et al., 2024, 2021; von Matt et al., 2024; Sarhadi et al., 2023; Wu et al., 2022), or the focus is on either the propagation of meteorological drought to other drought types, the co-occurrence of only two drought types (e.g. Hao et al., 2025; Wu et al., 2022), or the compounding of drought with other extremes such as heatwaves (e.g. Li et al., 2025). To our knowledge, there are only a few studies addressing the compounding of at least the three most common drought types (meteorological, hydrological, agricultural) on a global scale. Ahopelto et al. (2020) analysed the probability of compounding of different drought type combinations over the period 1981–2010. Kallio et al. (2019), estimated compound droughts globally using ten different drought indices and data from the Earth System Data Lab (Mahecha et al., 2020) over the relatively short time period 2004–2011. More recently, Hao et al. (2025) assessed multivariate, preconditioned, and temporally and spatially compounding droughts using several drought indices with the aim to improve monitoring of compound droughts – however, their reported assessment of the global multivariate droughts cover only the year 2022 and two drought indices.

The issue of compounding drought types is adjacent to many types of drought analyses. First, there is a substantial corpus of analyses of drought propagation from precipitation through the hydrological cycle. For instance, Yang et al. (2024) investigate drought propagation through the lens of multivariate compound droughts in China, finding that spatial and temporal features of drought events are essential factors in understanding compound drought evolution. Zhang et al. (2022) highlight that drought propagation is influenced by catchment characteristics and indicator choice. Second, multivariate drought indices share similarities with multivariate compound drought analysis, both of which integrate information across multiple compartments of the hydrological cycle. As an example, the Grand Mean Index (GMI; Mo and Lettenmaier, 2014) integrates precipitation, soil moisture and runoff output over multiple land surface models to provide an 'objective' estimate of drought severity across hydrological compartments. Third, finding proxies among drought indicators aim to identify indicators with strong correlation and similar occurrence of drought events has similarities with multivariate compound drought analysis. For example, Baez-

https://doi.org/10.5194/egusphere-2025-3909
Preprint. Discussion started: 3 September 2025

Villanueva et al. (2024) analysed how meteorological, soil moisture and snow drought indices coincide with hydrological drought in Chile and found that the best proxies vary based on catchment characteristics.

Although these studies have substantially improved the understanding of the compound droughts, they are restricted by their incomplete coverage of drought types and/or their limited temporal or spatial coverage. Currently, no global study exists that consistently assesses the compounding of meteorological, agricultural and hydrological droughts at a daily resolution within a multi-model framework, which is crucial for understanding their patterns and dynamics.

In this paper, we therefore address this research gap by identifying the spatial patterns and temporal trends of the compound drought events, where meteorological, agricultural, and hydrological droughts co-occur, to identify regions most at risk. Using hydrological datasets from global hydrological models (GHMs) with daily temporal and 0.5° spatial resolution for the period 1961–2020, we compute empirical standardised drought indices for precipitation, soil moisture and river discharge to cover each drought type, respectively. Further, we add to the discussion of uncertainty in global drought estimates through an analysis of uncertainty in the ensemble of nine estimates from the Inter-Sectoral Impact Model Intercomparison Project experiment 3a (ISIMIP, Frieler et al., 2024).

2 Data and Methods

The overall workflow for our study is shown in Figure 1. We describe the ISIMIP data used in Section 2.1. Section 2.2 describes how we compute the empirical drought indices (Fig. 1A), followed by our approach to event characterisation based on run theory in Section 2.3. Section 2.4 explains how we identify compound events, based on ensemble median of the nine members of our ensemble (Fig. 1B) and an alternative method based on events of individual drought types (Fig. 1C). Finally, Section 2.5 details our trend analysis, and Section 2.6 outlines an analysis based on El Niño Southern Oscillation (ENSO, Fig. 1D).

https://doi.org/10.5194/egusphere-2025-3909
Preprint. Discussion started: 3 September 2025

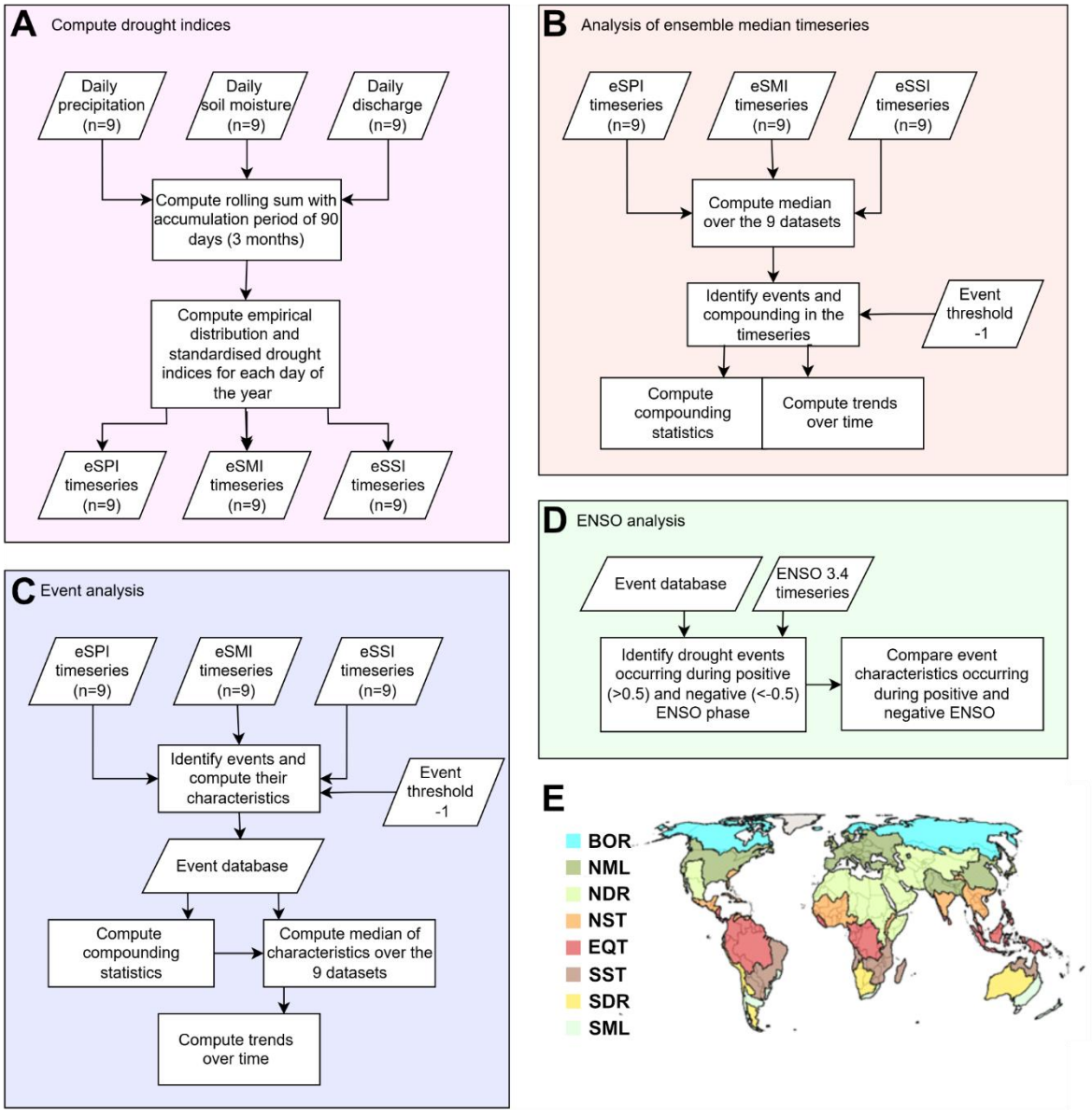

Figure 1. Workflow of our analyses. Panel A shows the workflow to compute the empirical drought indices. Panel B gives the workflow based on the ensemble median timeseries, panel C shows the workflow based on analysis of identified drought events, and panel D for the ENSO analysis. Panel E shows the global hydrobelts we use to summarise our results.

5

2.1 Data

We used data from the ISIMIP experiment 3a, consisting of historical model runs based on reanalysis forcing datasets. We selected all model runs which met the following criteria: 1) model is run with historical human forcing; 2) no sensitivity

https://doi.org/10.5194/egusphere-2025-3909
Preprint. Discussion started: 3 September 2025

experiment (i.e., the model runs are based on observed climate and human activity patterns – see Frieler et al., 2024); 3) model output includes soil moisture and discharge; and 4) output is of daily temporal resolution. When the ISIMIP data repository was accessed on 5th September 2024, there were a total of 9 model runs that satisfied these criteria. The three models were WaterGAP 2.2e (Müller Schmied et al., 2023), MIROC-INTEG-LAND (Yokohata et al., 2020), and H08 (Hanasaki et al., 2018). Each model was forced with three climate forcing datasets: 20CRv3-ERA5, 20CRv3-W5E5, and GSWP3-W5E5 (Frieler et al., 2024). We used daily precipitation data from the three reanalysis climate datasets used to force the GHMs.

To summarise the results on a global scale, we used the global hydrobelts (Meybeck et al., 2013). 'Hydrobelts' refer to hydrologically similar regions and are based on hydrometeorological and climatic similarity. The nine hydrobelts are Ice, Boreal (BOR), Northern Mid Latitude (NML), Northern Dry (ND), Northern Sub Tropical (NST), Equatorial (EQT), Southern Sub Tropical (SST), Southern Dry (SD), and Southern Mid Latitude (SML) (see Figure 1E). We exclude ICE from the analysis, as it only exists in Greenland and we do not analyse glacier evolution in this study.

2.2 Computing empirical drought indices

We computed daily drought indices for meteorological, soil moisture and hydrological drought based on empirical distributions. We chose to use empirical distributions instead of fitting theoretical distributions for two reasons: First, based on our tests, the optimal theoretical distribution changes according to location and time of the year, and second, to base our analysis on single standard workflow required for efficient comparisons between regions (Van Loon, 2015). We fit the empirical distribution for each day of the year (365 empirical distributions for each grid cell, for each of the nine GHM model runs and for each variable) using values occurring within a seven-day window centred on the day. For example, when fitting a distribution for precipitation on 15th January, all values occurring between 12th and 18th of January in all years were included. The fitting of empirical distribution was done for the period 1961–1990 (and applied to the full analysis period 1961–2020), meaning that each distribution is based on 210 values. Furthermore, we used a 3-month accumulation period for each variable (precipitation, soil moisture and discharge). The accumulation period refers to the time period over which the data is summed for the calculation. This makes the standardised drought indices resilient to rapid daily or weekly variation in the timeseries. With an empirical distribution computed, we then estimated a standardised drought index (McKee et al., 1993) by forcing the empirical distribution into a standard normal distribution.

The drought indices we use in the study – empirical Standardised Precipitation Index (eSPI, meteorological drought), empirical Standardised soil Moisture Index (eSMI, agricultural drought) and empirical Standardised Streamflow Index (eSSI, hydrological drought) – are interpreted in the same way as any other standardised drought index, with negative values indicating drier and positive values indicating wetter-than-average conditions. The index value describes how many standard

https://doi.org/10.5194/egusphere-2025-3909
Preprint. Discussion started: 3 September 2025

deviations away a data point is from the mean. Commonly, index values below -1 are considered 'moderate', values under -1.5 'severe', and values under -2 are considered 'extreme' droughts.

2.3 Event characterisation

We identified drought events by using run theory, as developed by Yejyevich (1967). Through this approach, we computed the drought event duration (D), intensity (I) and severity (S) by examining values that fall below a predetermined threshold, which we set as -1, indicating a moderate drought (McKee et al., 1993). The duration of a drought event reflects the number of days the index value stays below a threshold. Intensity, in turn, refers to the mean index value throughout the event, while severity is the sum of the index values over the drought event. In this research, we did not, however, analyse event intensity or severity, but rather focused on compound event occurrence and duration.

On some occasions, the drought index values sunk below our event detection threshold of -1 for only a short duration (a few days, for instance). A common practise is to remove events shorter than some chosen cutoff duration. However, our approach was to combine separate events if there were less than 30 days between the end of the previous event and the start of the subsequent event. This limited the number of events in periods where the index value hovered around the threshold for extended periods by considering them a single event, without the need to remove short duration events. There are two reasons we chose 30 days (one month) as the threshold for combining events: 1) the majority of global studies on droughts are conducted with a monthly temporal resolution, making one month a natural choice; and 2) our chosen accumulation period for the drought indices is 90 days (three months), so any drought events occurring within 30 days from one another are not independent in any sense (strictly, this applies to any consequent events occurring within the full accumulation period of 90 days).

2.4 Identifying compound drought events and their probability of occurrence

We employed two methods for the identification of compound drought events. In the first method (Figure 1B), we computed the ensemble median of the nine timeseries of eSPI, eSMI and eSSI, and for each day we counted how many median indices (none, one, two or three) were simultaneously below the event threshold. We then used the run theory to identify periods when at least one, two or three drought types co-occurred simultaneously. This allowed us to compute the probability of occurrence of compound drought events for each 0.5° grid cell separately using eq. 1,

$$P_{compounding} = \frac{n_{compound\ events}}{n_{events}} \quad (1)$$

https://doi.org/10.5194/egusphere-2025-3909
Preprint. Discussion started: 3 September 2025

where $P_{compounding}$ is the probability of occurrence of a compound event, n_{events} is the number of events in the cell with at least one drought type below the threshold, and $n_{compound\ events}$ is the number of events where all three drought types co-occur simultaneously.

The second method is based on drought events identified with the run theory for each of the three drought indices. We compared the dates of individual events to the dates of events of other drought types and deemed a single drought event as a compound drought event if, during its duration, all three drought types occurred simultaneously. This allowed us to analyse each drought type separately and assess the probability of compounding conditional to a certain drought type.

2.5 Trends

To estimate the temporal trends in compound drought events, we computed Sen's slope (Sen, 1968), due to the large variation in the timeseries of the variables. Sen's slope is estimated as the median of the slope between pairs of data points, giving a robust estimate of the slope. We used Sen's slope for all timeseries trend computation, including timeseries and gridded data. Note that we excluded the year 1961 from trend computations, because the 3-month (90-day) accumulation period used to compute the drought indices resulted in fewer observations for that year compared to others. For trends computed based on drought events, each event was assigned to the year of the starting date in cases where the drought period covered multiple years.

2.6 ENSO analysis

We analysed the influence of ENSO on the duration of compound drought events on our dataset, due to its known influence on simultaneous droughts across the globe (e.g. Singh et al., 2021, 2022). We compared the monthly Niño 3.4 index timeseries obtained from the NOAA (2025) and matched drought events occurring during different phases of ENSO. We used a threshold value of 0.5 or above for La Niña, and -0.5 or below for El Niño events, following the approach used by Singh et al. (2022). After matching drought events to the ENSO phase, we took the median of the durations of the events and computed the difference between El Niño and La Niña events.

https://doi.org/10.5194/egusphere-2025-3909
Preprint. Discussion started: 3 September 2025

3 Results

3.1. Compound drought (event) characteristics

We first assessed the different characteristics of compound droughts over the study period (1961–2020) (Figure 2). We found that Southern Europe, East Asia, Indonesia, Central Africa, and Western South America stand out with the highest compound drought day count (annual average over the study period); in these regions, the count on average stayed above 25 days (Figure 2A). The trend over years from 1961 to 2020 (Figure 2C) showed high heterogeneity, but in general the trend was positive (i.e., drought day count increased) in the same areas as where the compound drought days per year were high. The most notable areas with a negative trend (i.e., days with smaller count) were found in Eastern USA, the Sahel, Northern India, and Siberia.

When assessing the median durations of compound drought events (based on outputs from all 9 forcing-model combinations over 1961–2020), we found that Equatorial regions experienced the longest event durations, even exceeding 70 days in Central Africa (Figure 2B). Primarily median durations remained below 50 days, and the lowest durations occurred in India, the Sahara, Northern Australia, and parts of Siberia. The global median duration of a compound drought event was 42 days. The change pattern in the median event durations (Figure 2D) was similar to the pattern of day count change (Figure 2C), though with some distinct differences. Parts of central sub-Saharan Africa and the Amazon Basin experienced very large increases (i.e., longer median duration) while parts of Tibet, Eastern North America, and Nordic countries experienced decreasing duration.

To understand the probability of compound droughts – i.e., when all three drought types co-occur in time and space – we identified all periods of the timeseries when at least one of the three drought types occurred. If at any point in this period all three drought types co-occurred, the event was categorised as a ‘compound event’. The highest probability (>30%) occurred in various monsoon weather systems (Eastern Africa, South and East Asia), as well as in other weather systems such as Mediterranean, the Andes, and Eastern Australia (Figure 2E). This indicates that in these areas the risk for one drought type to propagate to a compound drought was higher.

Finally, we assessed how ENSO impacts the co-occurring of these three drought types by assessing the difference of compound drought event durations between El Niño and La Niña (Figure 2F). Our results show that in areas along the coasts of the South Pacific Ocean, the Western and Southern parts of Africa, Southeast Asian islands, and most of Australia, the compound drought durations tended to be longer during El Niño than La Niña months. In turn, the durations were longer during El Niña months primarily in Northeastern Africa, Middle East, and eastern South America.

https://doi.org/10.5194/egusphere-2025-3909
Preprint. Discussion started: 3 September 2025

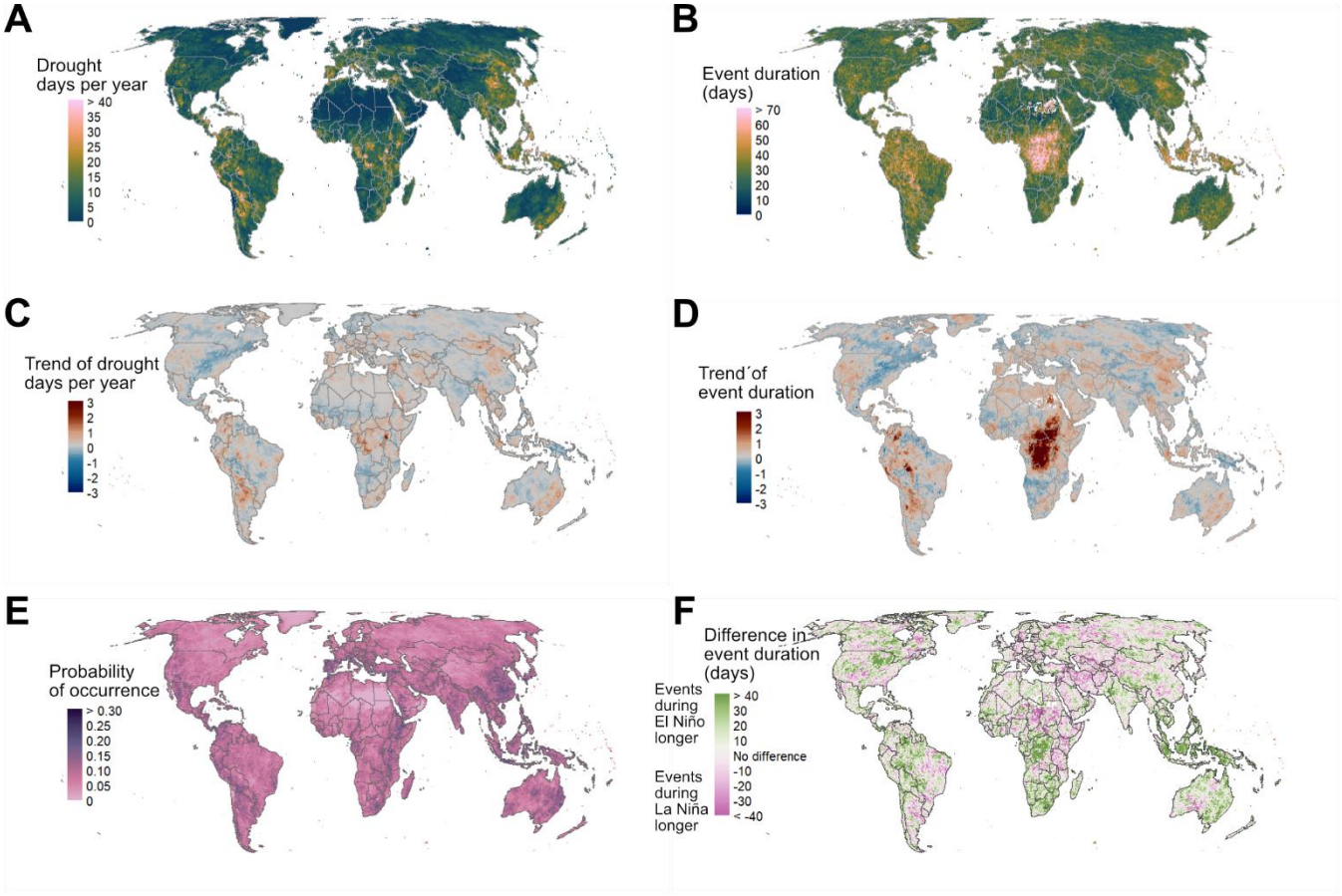

Figure 2. Mean (A) and the trend (C) of annual compound drought days with all three drought types co-occurring. Median of compound drought event duration (B) and its trend (D). Probability of the co-occurrence of all three drought indices (E). The difference in compound drought event duration between events occurring during El Niño and La Niña (F). Values mapped in tiles A, B, E are computed for the ensemble median for years 1961–2020. Trends are calculated using Sen's slope method.

3.2. Trends across hydrobelts over 1961–2020

To compare the temporal patterns across different hydrological regions, we aggregated the compound events at the scale of hydrobelts (map in Figure 1E). In general, the trend for days under compound drought per year increased in all hydrobelts apart from the boreal hydrobelt (Figure 3A), though the trend was particularly steep in the equatorial and southern mid-latitude hydrobelts. It should be noted that the different GHM-forcing data combinations showed high variability. The mean annual index value (Figure 3B), in turn, shows somewhat more varying patterns. The aggregated index values for each hydrobelt showed a mostly negative trend, signifying a general drying pattern according to all three drought indices. The boreal hydrobelt stands out as the only one with a significant wetting trend and therefore increasing mean annual index values. The northern

https://doi.org/10.5194/egusphere-2025-3909
Preprint. Discussion started: 3 September 2025

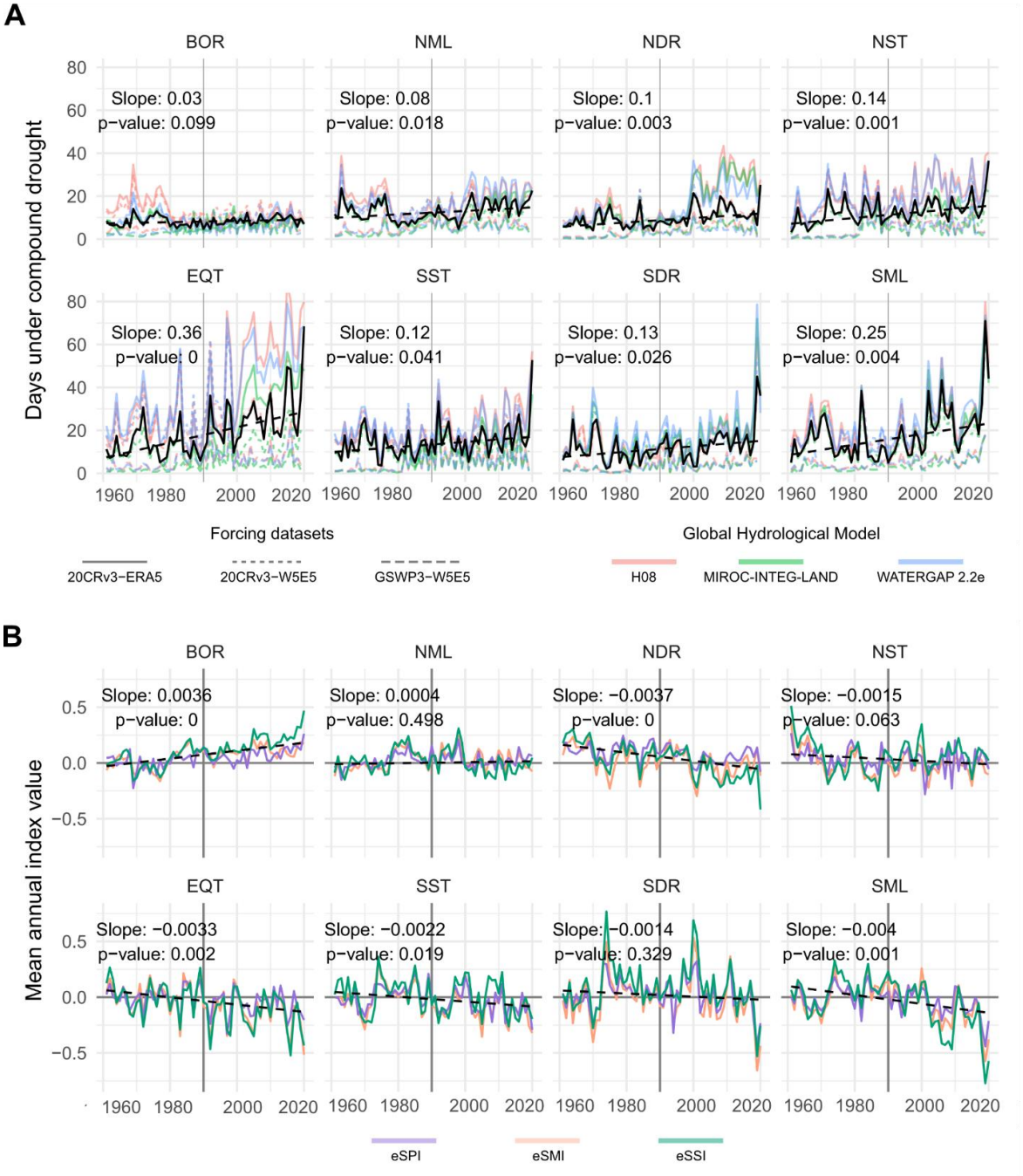

Figure 3. Panel A shows the mean number of days under compound drought over the hydrobelts as identified from the different model runs and the ensemble median. Panel B shows the mean annual index value for the three drought indices and all hydrobelts as computed from the ensemble median as well as the combined trend over the three drought indices. The vertical bar denotes the year 1990, which is the last year used to fit the empirical distribution. Note that a positive slope in panel A signifies increasing compound drought occurrence, while a negative trend in panel B signifies a general drying trend. eSPI stands for empirical Standardised Precipitation Index, eSMI for empirical Standardised soil Moisture Index, and eSSI for empirical Standardised Streamflow Index.

https://doi.org/10.5194/egusphere-2025-3909
Preprint. Discussion started: 3 September 2025

mid-latitude did not show any trend, and in northern sub-tropical and southern dry hydrobelts, the negative trend was statistically uncertain. The steepest decreases in the value can be found in northern dry, equatorial and southern mid-latitude hydrobelts. Interestingly, although the equatorial hydrobelt showed the fastest increase in compound drought days (Fig 3A), the general drying trend was stronger in northern dry and southern mid-latitudes.

These findings indicate that, on average, compound drought events have become more frequent and more intense. Figure 3B also shows that the three drought indices were generally in sync over the years. For instance, in the equatorial and southern dry hydrobelts, the index values were more closely aligned compared to other hydrobelts. The clearest deviations can be found in the boreal hydrobelt, where eSSI index shows larger wetting than eSMI or eSPI since 2004, and in the northern dry hydrobelt, where eSSI showed the largest drying trend. By comparing Figures 3A and B, we can see that the number of compound drought days follow the annual index values. For instance, northern mid-latitudes showed a smaller number of compound dry days between 1980 and 2000, while at the same time the aggregated index values indicated a generally wetter period. A Pearson correlation coefficient of -0.77 computed globally showed a strong association between the mean of eSPI, eSMI and eSPI index values, and the number of drought days (i.e., as the index values decrease toward more dry conditions, the number of compound days increases).

3.3. Compound events from the lens of specific drought types

Next, we explored the duration, probability, event count of compound drought events, and the proportion of compound drought periods through the lens of each drought type. This means that after the drought events for each index were recognised, they were compared to events of other indices to identify compounding. Here, we used each drought type as the basis of computation, which is the drought type that persists throughout and to which the co-occurrence of other two types are compared.

Overall, we found that eSPI drought event characteristics differ from the eSMI and eSSI events with similar characteristics to one another, as summarised in Table 1. We found almost twice as many eSPI drought events per grid cell as eSMI or eSSI events, with median durations around half as long. Only 20% of eSPI events had periods with co-occurring eSMI and eSSI events, which was considerably less than the 36% and 34% for eSMI and eSSI, respectively. When an eSPI event is categorised as a compound event, on average the compounding period covers a larger proportion of that event than for eSMI or eSSI.

https://doi.org/10.5194/egusphere-2025-3909
Preprint. Discussion started: 3 September 2025

Table 1. Global mean drought characteristics over 1961–2020. eSPI stands for empirical Standardised Precipitation Index, eSMI for empirical Standardised soil Moisture Index, and eSSI for empirical Standardised Streamflow Index.

Index	Events per cell	Median duration (days)	Probability of compounding	Proportion of compounding
eSPI	79	42	20%	59%
eSMI	40	96	36%	41%
eSSI	42	83	34%	42%

We found that in the boreal hydrobelt and a large part of Asia, drought events with eSMI (Fig 4C) lead to compound drought more often than events of eSPI (Fig 4A) or eSSI (Fig 4E). Conceptually, this is expected if we think of a linear progression from rainfall deficit to soil moisture deficit, and finally to low river discharges. eSMI is conceptually located in the middle between the start and the end of the propagation, and the conceptual distance from eSPI to eSSI and vice versa is larger leading to lower probability of simultaneous occurrence. However, actual drought propagation is not necessarily linear and is influenced by catchment properties (Yang et al., 2024; Zhang et al., 2022), and thus eSSI events are most likely to contain compound drought periods in much of Latin America, Eastern North America, Northeastern Europe, Sub-Saharan Africa and insular Southeast Asia. We therefore found that eSPI events were least likely to lead to compound droughts. This is further evident in the bar plots in Fig 4G: we identified a significantly larger event count for eSPI than for eSMI or eSSI. The smallest difference in event counts was in the southernmost hydrobelts, with the difference increasing the further north we went. eSPI events had a lower probability of compounding than the other two indices, with 25% of events in the equatorial hydrobelt and just 17% in the boreal hydrobelt containing a compound drought period.

https://doi.org/10.5194/egusphere-2025-3909
Preprint. Discussion started: 3 September 2025

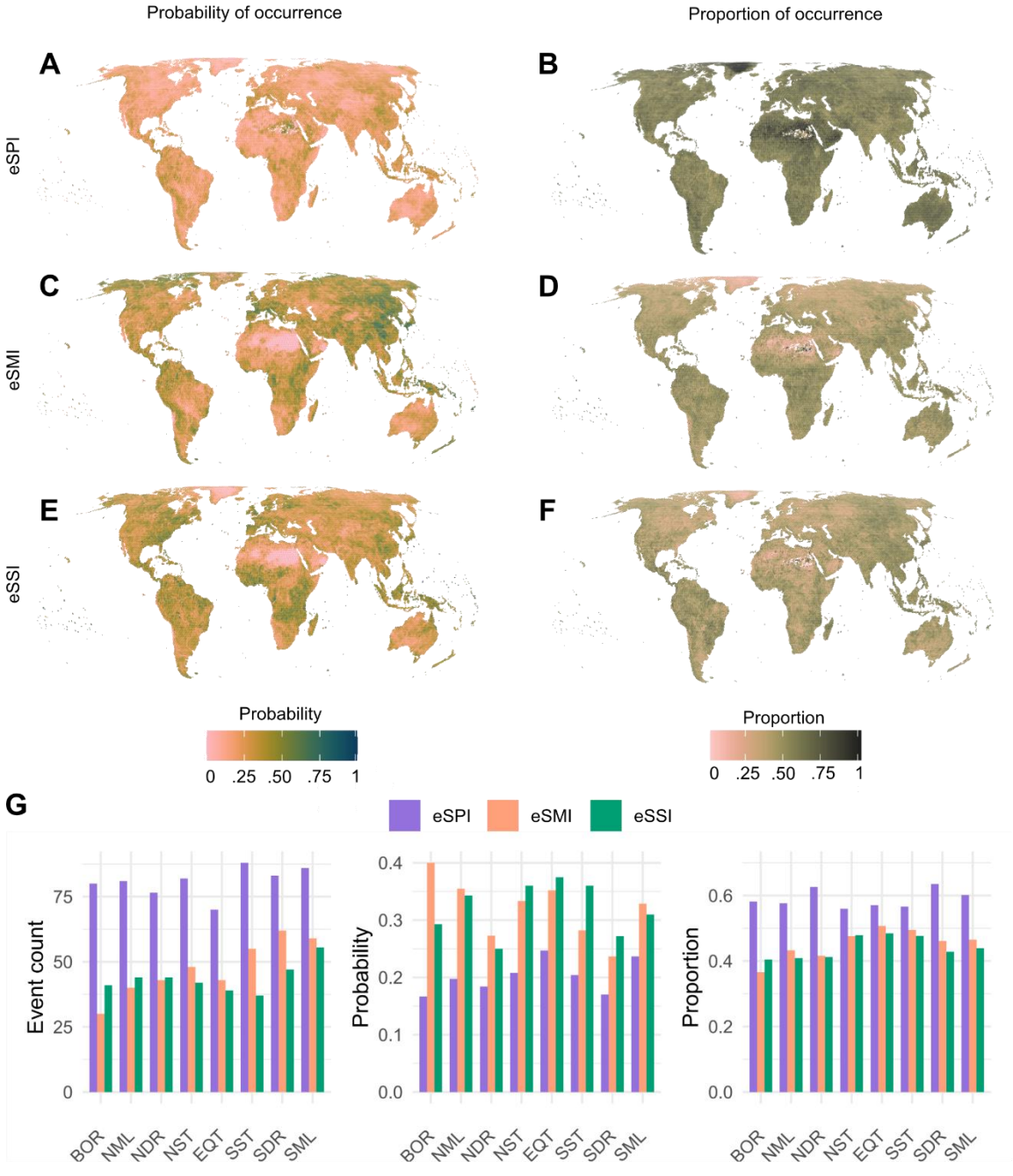

Figure 4. Compound drought event occurrence under specific drought types (i.e., the compound droughts conditional on a specific type). Panels A, C and E show the median probability of occurrence of eSPI, eSMI and eSSI events, respectively, whereby all three drought types co-occur simultaneously. Panels B, D and F shows the mean of the proportion of compound drought period over the entire drought event duration of eSPI, eSMI and eSSI, respectively. Panel G displays a summary of the global patterns of event counts, probability of a drought event of a specific type also containing compound drought, and the proportion of compounding (compound drought period over the entire drought event), each aggregated to hydrobelts. The values in panel G are medians over the 9-member ensemble. eSPI stands for empirical Standardised Precipitation Index, eSMI for empirical Standardised soil Moisture Index, and eSSI for empirical Standardised Streamflow Index.

https://doi.org/10.5194/egusphere-2025-3909
Preprint. Discussion started: 3 September 2025

We then assessed the proportion of the drought event covered by the compounding period, when the event is classified as a compound drought event and shows that the compounding periods covered a much larger proportion of eSPI events all across the globe than they did for eSMI or eSSI events (Figs 4B, D, F). This was particularly true for arid regions across the globe. The proportion was in general larger for eSMI events than they were for eSSI events, but there were some locations where the opposite was true – Southern Brazil, parts of Central America and parts of boreal and northern mid-latitudes hydrobelts. These findings are echoed in the bar plots of Figure 4G: eSPI clearly deviates from eSMI and eSSI. The smallest differences were in the equatorial and both northern and southern subtropical hydrobelts and increased as the latitude distances from the equator.

We also computed the Pearson correlation coefficient between compound drought event counts and probability of compounding and found that there was a moderate negative correlation (-0.44) between event counts and probability of compounding. Generally, a smaller event count means longer individual events, because of our methodological choice of using an empirical distribution and a threshold to detect drought events. This choice means that there are approximately equal number of drought days over 1961–1990 in every grid cell, with deviations only in the latter period 1991–2020 if the distribution changes. Longer drought durations naturally increase the likelihood of observing simultaneous drought types compared to shorter drought durations. We also found a moderate positive correlation (0.62) between event counts and the proportion of compound drought period over the event duration, meaning that increasing event counts (shorter drought event durations) lead to an increasing proportion of compounding.

4 Discussion

4.1 Comparison to literature

In this study, we provide the first comprehensive global analysis of compound droughts, considering all three main drought types, over the past decades. Our work thus considerably extends the existing literature on global analyses that consider either only two indices and only report results on droughts in one year (soil moisture and vapor pressure deficit for 2022, Hao et al., 2025), consider only very short time period (2003–2010, Ahopelto et al., 2020), or consider only pairwise occurrence of compound droughts (Kallio et al., 2019). Although direct comparison is not possible due to differences in methods and temporal resolution, some insights can be drawn. Ahopelto et al. (2020) found that the compound drought trends in southern sub-tropical and southern dry hydrobelts contrast those of the other hydrobelts, while we found that these two hydrobelts do not particularly stand out from others (Figs 3A and 4G); it should be noted, however, that our results are based on substantially longer timeseries than that of Ahopelto et al. (2020). Kallio et al. (2019) found that meteorological drought co-occurs with hydrological drought 43.6% of the events, and with agricultural drought 47.0% of the events. These are higher percentages compared to the results of our study (33.3% and 34.4%), though the pattern is similar as meteorological with agricultural drought occurs slightly more frequently than meteorological with hydrological drought.

https://doi.org/10.5194/egusphere-2025-3909
Preprint. Discussion started: 3 September 2025

Results shown in Figure 3 for the boreal hydrobelt show a trend of wetting, no increase in compound droughts, and generally drying trends in most other global hydrobelts. This matches the observations by Vieira and Stadnyk (2023), who assessed the trends in hydrological droughts among an ensemble of global climate models. They found that northern latitudes show evidence of shorter, less intense droughts, while large portions of other global land areas are drying – though, in significant portions of these land areas, no clear trend is detected. Our results fit this observation as well; aggregated to hydrobelts, we found no significant trend in wetting, drying, or in compound drought occurrence over northern mid-latitudes or in southern dry, and a drying trend elsewhere. Our analysis further shows that the compounding of the three drought types has become more common in most hydrobelts over the last six decades. Other literature also supports this finding, stating that compound droughts are becoming more frequent globally due to climate change (von Matt et al., 2024). These patterns are further confirmed by Porkka et al. (2024) who used ISIMIP 2b data (the previous round of experiments to our study using ISIMIP 3a) to investigate how streamflow and soil moisture percentiles deviate from a pre-industrial baseline. Their results showed a wetting trend, particularly for soil moisture, in the high latitudes and a generally drying trend across most of the other global land area.

In a study based on satellite observations of Terrestial Water Storage (TWS), Chandanpurkar et al. (2025) suggested that the high latitude areas (mainly boreal hydrobelt) are drying over the most recent two decades (2002–2024). TWS measures contain all stored water, including glaciers and permafrost, which are not a component of our study. As water stored in ice melts, the water is released into the landscape and will appear as increased soil moisture and streamflow, which is reflected in our results for the boreal hydrobelt (Figure 3B). For TWS, however, the signal decreases when the moisture released from ice evaporates or gets transported away as streamflow. We should note, however, that we provide our results over 1961–2020, while Chandanpurkar et al. (2025) consider more recent trends over 2002–2024.

Comparing our findings to more local studies, Wu et al. (2022) studied the propagation of meteorological drought to hydrological drought in South China, using observed hydrological data from years 1960 to 2015. They also use SPI and SSI indices and run theory to identify drought events. The main difference between their analysis and ours lies in the definition of drought events: they defined a drought event as a period during which the drought index time series (i.e., SSI or SPI) remains below zero for at least three months, whereas in our study, a drought event was defined as a period when the indices fall below –1. Their results showed that most compound drought events lasted less than three months, which matches our results showing durations below two months in South China as well as globally.

4.2 Uncertainty in the ensemble

Numerous studies have shown that global hydrological modelling has high uncertainties arising from poor data quality, difficulty in addressing human impact on a global scale, and selecting appropriate model structures and parameters (Reinecke et al., 2025). Selection of drought indices bring additional uncertainties due to their subjectivity and because the relationship

https://doi.org/10.5194/egusphere-2025-3909
Preprint. Discussion started: 3 September 2025

between drought indices can differ between regions. For instance, Afshar et al (2022) reported that SPI generally correlates better with soil moisture drought in northern and SPEI in the southern hemisphere. Figure 5A shows the global patterns between the probability of compounding (conditional on any drought type) and the coefficient of variation in the probability within our ensemble of nine estimates. The bivariate map shows that large uncertainties can be found everywhere in the world, particularly in deserts and drylands, boreal hydrobelt and in the tropics. This variability is likely due to model structure and/or global parametrisation not being able to represent hydrological processes in drylands (see, for example, Quichimbo et al., 2021). Our chosen empirical drought indicators are also not optimal for the purpose; if, for instance, streamflow timeseries contains more than 16% of zero-flow days, eSSI with a drought threshold of -1 will never be able to detect a drought. In areas with a significant number of zero-flow days, a different drought index could reduce this uncertainty (Cammalleri, 2024).

Disagreement and uncertainty within the ensemble are clearly visible in Figure 5B, which shows how the probability of compounding varies across hydrobelts and different sizes of drainage basins. All the ISIMIP model runs showed that the probability decreases as basin size increases. This is due to the increasing heterogeneity in the conditions within large basins compared to smaller ones, as well as attenuation and propagation of the precipitation to hydrological drought. However, from the plots in Figure 5B, it is clear that model runs forced with GSWP3-W5E5 resulted in substantially smaller probability of compound droughts. The same applies for available runs with the global hydrological model MIROC-INTEG-LAND. The simulations with models H08 and WaterGAP 2.2e agree with one another across most hydrobelts, though it should be noted that H08 shows significantly larger probability of compounding in the boreal hydrobelt (Figure 5B).

Figure 5C shows a timeseries of the streamflow percentiles, with clearly visible issues in Central Africa (0.25° N, 23.25° E, falling in the Equatorial Hydrobelt). ERA5 precipitation is known to have problems in the tropics (e.g. Lavers et al., 2022; Rivoire et al., 2021). Starting from approximately 1998, the streamflow percentiles begin to decline, and by 2005 for all three assessed GHMs forced with 20CRv3-ERA5 mostly output streamflow that is below the lowest simulated streamflow within the calibration period 1961–1990. Input forcing from 20CRv3-W5E5 and GSWP3-W5E5 does not suffer from the same behaviour – however, from the percentile timeseries, these model outputs are also anomalous with very little interannual variation from 1998 to 2020. Keune et al. (2025) recently published a global drought dataset derived from ERA5 data, which includes SPI, and the Central African anomaly we observe is not present in their dataset. They fit their distribution to a different period (1990–2020) and use ERA5 data directly, rather than the adjusted dataset from ISIMIP3a. The very high trend is also visible in the study by Gebrechorkos et al. (2025) for Standardised Precipitation and Evapotranspiration Index, based on

https://doi.org/10.5194/egusphere-2025-3909
Preprint. Discussion started: 3 September 2025

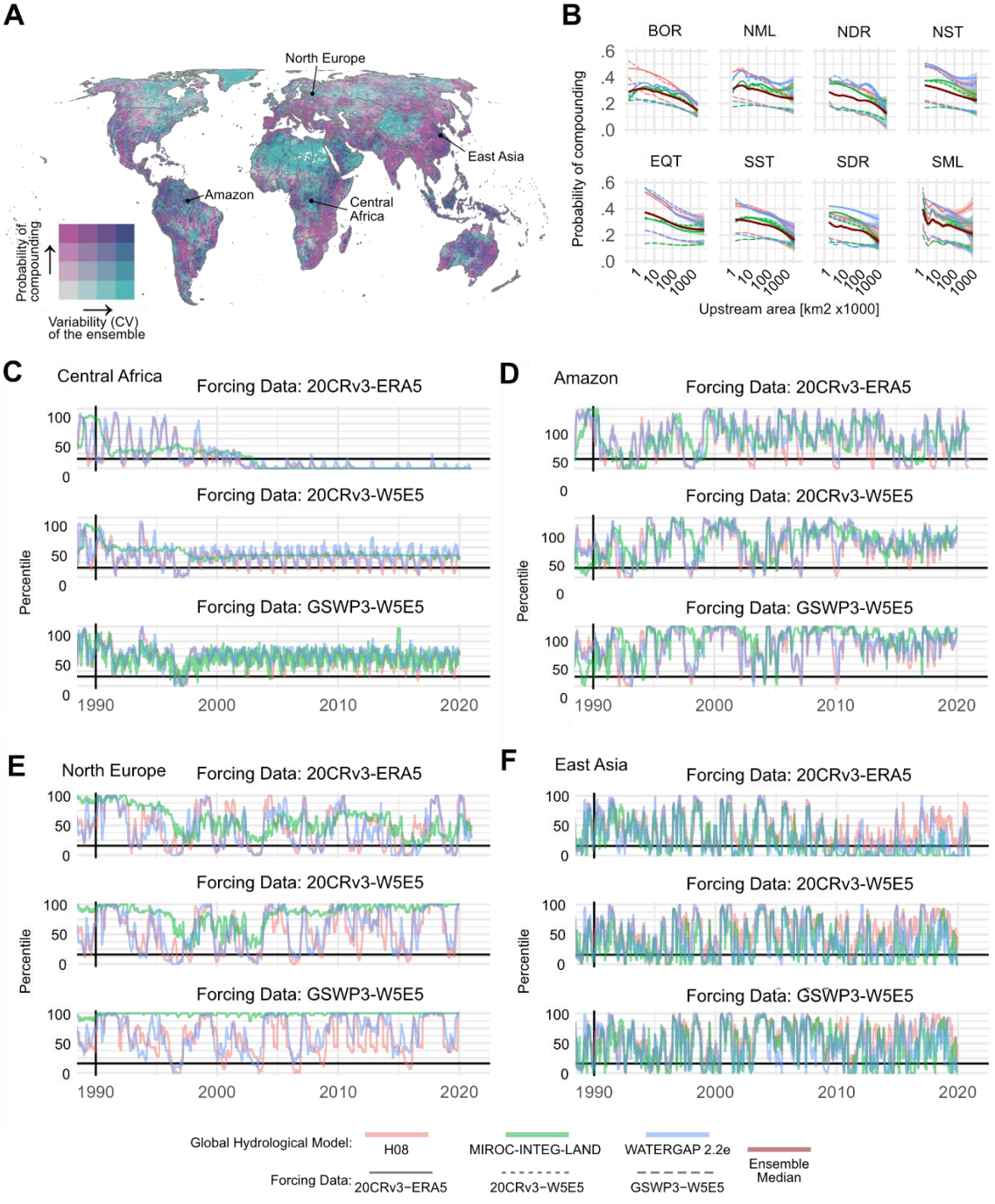

Figure 5. Uncertainty of the compound droughts within the ensemble. Panel A shows a bivariate map between the ensemble median probability of compounding and its coefficient of variance within the ensemble. Panel B shows how the probability of compounding varies between hydrobelts, basin size, model and forcing datasets. Panels C–F show timeseries of percentiles from the empirical distribution for four locations indicated in Panel A, shown for all GHMs. The panels are separated by the forcing data used to run the GHMs. The vertical bar in the timeseries denotes 1990, which ends the period 1961–1990 used to train the empirical distributions. The horizontal bar denotes the drought threshold used in this study.

https://doi.org/10.5194/egusphere-2025-3909
Preprint. Discussion started: 3 September 2025

CHIRPS (Funk et al., 2015) and MSWEP (which includes ERA-Interim, the predecessor of ERA5, as well as CHIRPS as a part of its components; Beck et al., 2019) climate data. Nonetheless, the anomaly we observe here pushes our results in Central Africa higher and are likely not truly valid for this region. This influence is also seen in the trends in Equatorial Hydrobelt: past 1998, the number of days under compound drought increased sharply for 20CRv3-ERA5 forced models and thus pushes the median and the trend line higher.

Figures 5D–F shows the same timeseries of streamflow percentiles as in Figure 5C, but for different locations each displaying different behaviour of the set of estimates. In the Amazon (Figure 5D, 0.25° N, 57.75° W), the climate forcing datasets show similar pattern throughout 1991–2020, with model runs forced by 20CRv3-ERA5 giving the lower and simulations forced with GSWP3-W5E5 higher values than others. Here, streamflow simulated by MIROC-INTEG-LAND is slower to react to changes in forcing than those simulated by H08 and WaterGAP 2.2e. In Northern Europe (Figure 5E, 58.25° N, 31.25° E), streamflow simulations from MIROC-INTEG-LAND model are much slower to react than the other two models, and where model runs forced with 20CRv3-ERA5 shows more realistic behaviour. In East Asia (Figure 5F, 33.25° N, 117.25° E), all three GHMs in the ensemble show similar behaviour across all three climate forcing datasets, with the only exception being the period after 2010, where streamflow simulations modelled with H08 are somewhat higher than the other two models. These plots show large differences between the ensemble members and shows that the relationship between the models is nonstationary across different regions.

We report a major spread of compound drought estimates among the ISIMIP ensemble members. The uncertainty is particularly evident in Central Africa and elsewhere in the tropics, but we showed that the behaviours of the models and the climate forcing datasets differ elsewhere too. Future analysis of multivariate compound droughts covering all major hydrological compartments would benefit from global hydrological modelling targeting drought representations in particular, or other methodological techniques to improve drought representation on a global scale. Analysing the specific reasons for which different GHM and climate forcing combinations result in such different compound drought characteristics is beyond the scope of this paper (see Tiwari et al. ,2025 for an analysis of the differences between global water models). Reinecke et al. (2025) provide insights into how hydrological modelling could be improved to reduce uncertainties. Understanding how drought propagation behaves in GHMs in different regions and under different conditions could also help refine the estimates (Zhang et al., 2022). Furthermore, drought-specific model averaging techniques may also improve drought representation in GHM ensembles (such as Shakeel et al., 2025).

https://doi.org/10.5194/egusphere-2025-3909
Preprint. Discussion started: 3 September 2025

4.3 Drought management and compound droughts

Current drought governance often focuses on individual drought types in isolation (e.g., meteorological drought), despite the need for integrated governance across drought types (Ahopelto et al., 2023). Our findings highlight the need to revise drought risk strategies and early warning systems to account for multi-dimensional, co-occurring droughts. In particular, policies that integrate agricultural, water resources, and energy planning may better address the cascading impacts of compound droughts across sectors. For example, such droughts pose significant challenges for energy systems like hydropower, which depends on a stable water supply (van Vliet et al., 2016). This has already led to electricity shortages in countries including Indonesia, Lao PDR, Ethiopia, and Brazil. Incorporating compound drought scenarios into integrated energy and water resource planning is therefore essential to mitigate cascading failures across the water–energy–food nexus (Bazilian et al., 2011; Howells et al., 2013).

Additionally, the uncertainties observed across global models in this study reinforce the need for adaptive governance mechanisms that can operate under incomplete information (Guillaume et al., 2017; Walker et al., 2013). Grounded in flexibility, scenario planning, and risk-based decision-making, such approaches may prove essential as climate change continues to increase the frequency and complexity of drought impacts globally.

5 Conclusion

In this study, we present the first global multi-model analysis of multivariate compound droughts, encompassing meteorological, agricultural and hydrological droughts. We examined the spatial patterns and temporal trends of compound droughts over 1961–2020. Our results revealed substantial spatial differences in compound drought occurrence. The most susceptible areas to compound droughts are in Southern Europe, East Asia, Insular Southeast Asia, Central Africa, and Western South America. Globally, the El Niño phase of ENSO contributes to longer compound drought events than the La Niña phase everywhere except for the Rift Valley area in Africa and in Western and Central Asia. There is a general drying trend across different hydrobelts, with the strongest increase in compound droughts in the Equatorial hydrobelt. The outlier in the pack is the Boreal hydrobelt, which is the only region showing a strong wetting trend and the lowest numbers of compound droughts. We also showed that different drought indices provide a different lens to understand compound droughts. There is, however, significant uncertainty in compound drought characteristics arising from different combinations of global hydrological models and forcing data used to run them.

Our results help to understand the dynamics and trends of compound drought by identifying frequency and duration. This understanding can support cross-sectoral drought preparedness actions and, for example, agricultural irrigation challenges when hydrological drought co-occurs with other drought types. The results also highlight the need to improve drought

https://doi.org/10.5194/egusphere-2025-3909
Preprint. Discussion started: 3 September 2025

adaptation, since the frequencies and durations have been increasing and are estimated to increase. The results also have important implications for anticipatory and cross-sectoral drought governance globally. By identifying regions where compound droughts are intensifying, this study supports the prioritisation of preparedness actions in some of the most vulnerable areas.

Acknowledgements

MKa and MKu were supported by Maa- ja Vesitekniikan Tuki ry, the European Research Council (ERC) under the European Union's Horizon 2020 research and innovation programme (grant agreement No. 819202), and the Research Council of Finland flagship project Digital Water (DIWA). AF and MKu were supported by GloWater project (365753) funded by the Strategic Research Council of Finland. PS gratefully acknowledges Sven Hallin Research Foundation sr for funding a EGU 2025 conference trip, and Finnish Environment Institute (Syke) for supporting her participation and making the trip possible. We wish to thank the ISIMIP and all contributing modelling teams for making this research possible. We also wish to acknowledge the Earth System Data Lab which provided the opportunity to develop the very first concept of this study back in 2018.

Code and Data availability

The model runs underpinning this research are openly available from the ISIMIP repository at https://data.isimip.org. The hydrobelts are available at https://doi.pangaea.de/10.1594/PANGAEA.806957. The code to reproduce the results and figures will be deposited in Zenodo upon acceptance of the manuscript.

Author contributions

MKa, LA, AF, PK, and MH designed the original concept of the study. MKa and Mku curated the data. MKa, Mku and PS designed the methodology, performed formal analysis, and prepared the original manuscript draft. MKa and PS wrote the code to perform the analyses. MKu provided the funding acquisition and supervision. All authors participated in writing and reviewing of the manuscript.

https://doi.org/10.5194/egusphere-2025-3909
Preprint. Discussion started: 3 September 2025

References

Afshar, M. H., Bulut, B., Duzenli, E., Amjad, M., and Yilmaz, M. T.: Global spatiotemporal consistency between meteorological and soil moisture drought indices, Agricultural and Forest Meteorology, 316, 108848, https://doi.org/10.1016/j.agrformet.2022.108848, 2022.

Ahopelto, L., Kallio, M., Heino, M., Kinnunen, P., Fallon, A., and Kummu, M.: Quantifying the co-occurrence of hydrological, meteorological, and agricultural droughts on a global scale, Copernicus Meetings, https://doi.org/10.5194/egusphere-egu2020-7960, 2020.

Ahopelto, L., Kallio, M., Veijalainen, N., Kouki, R., and Keskinen, M.: Drought hazard and annual precipitation predicted to increase in the Sirppujoki river basin, Finland, Climate Services, 31, 100400, https://doi.org/10.1016/j.cliser.2023.100400, 2023.

Alahacoon, N. and and Edirisinghe, M.: A comprehensive assessment of remote sensing and traditional based drought monitoring indices at global and regional scale, Geomatics, Natural Hazards and Risk, 13, 762–799, https://doi.org/10.1080/19475705.2022.2044394, 2022.

Baez-Villanueva, O. M., Zambrano-Bigiarini, M., Miralles, D. G., Beck, H. E., Siegmund, J. F., Alvarez-Garreton, C., Verbist, K., Garreaud, R., Boisier, J. P., and Galleguillos, M.: On the timescale of drought indices for monitoring streamflow drought considering catchment hydrological regimes, Hydrology and Earth System Sciences, 28, 1415–1439, https://doi.org/10.5194/hess-28-1415-2024, 2024.

Bazilian, M., Rogner, H., Howells, M., Hermann, S., Arent, D., Gielen, D., Steduto, P., Mueller, A., Komor, P., Tol, R. S. J., and Yumkella, K. K.: Considering the energy, water and food nexus: Towards an integrated modelling approach, Energy Policy, 39, 7896–7906, https://doi.org/10.1016/j.enpol.2011.09.039, 2011.

Beck, H. E., Zimmermann, N. E., McVicar, T. R., Vergopolan, N., Berg, A., and Wood, E. F.: Present and future Köppen-Geiger climate classification maps at 1-km resolution, Scientific Data, 5, 180214, https://doi.org/10.1038/sdata.2018.214, 2018.

Beck, H. E., Wood, E. F., Pan, M., Fisher, C. K., Miralles, D. G., Dijk, A. I. J. M. van, McVicar, T. R., and Adler, R. F.: MSWEP V2 Global 3-Hourly 0.1° Precipitation: Methodology and Quantitative Assessment, https://doi.org/10.1175/BAMS-D-17-0138.1, 2019.

Cammalleri, C.: A unified streamflow drought index for both perennial and intermittent rivers at global scale, Hydrological Sciences Journal, 69, 1848–1859, https://doi.org/10.1080/02626667.2024.2390925, 2024.

Chandanpurkar, H. A., Famiglietti, J. S., Gopalan, K., Wiese, D. N., Wada, Y., Kakinuma, K., Reager, J. T., and Zhang, F.: Unprecedented continental drying, shrinking freshwater availability, and increasing land contributions to sea level rise, Science Advances, 11, eadx0298, https://doi.org/10.1126/sciadv.adx0298, 2025.

Feng, G., Chen, Y., Mansaray, L. R., Xu, H., Shi, A., and Chen, Y.: Propagation of Meteorological Drought to Agricultural and Hydrological Droughts in the Tropical Lancang–Mekong River Basin, Remote Sensing, 15, 5678, https://doi.org/10.3390/rs15245678, 2023.

Frieler, K., Volkholz, J., Lange, S., Schewe, J., Mengel, M., del Rocío Rivas López, M., Otto, C., Reyer, C. P. O., Karger, D. N., Malle, J. T., Treu, S., Menz, C., Blanchard, J. L., Harrison, C. S., Petrik, C. M., Eddy, T. D., Ortega-Cisneros, K., Novaglio, C., Rousseau, Y., Watson, R. A., Stock, C., Liu, X., Heneghan, R., Tittensor, D., Maury, O., Büchner, M., Vogt, T., Wang, T., Sun, F., Sauer, I. J., Koch, J., Vanderkelen, I., Jägermeyr, J., Müller, C., Rabin, S., Klar, J., Vega del Valle, I. D., Lasslop, G.,

https://doi.org/10.5194/egusphere-2025-3909
Preprint. Discussion started: 3 September 2025

Chadburn, S., Burke, E., Gallego-Sala, A., Smith, N., Chang, J., Hantson, S., Burton, C., Gädeke, A., Li, F., Gosling, S. N., Müller Schmied, H., Hattermann, F., Wang, J., Yao, F., Hickler, T., Marcé, R., Pierson, D., Thiery, W., Mercado-Bettín, D., Ladwig, R., Ayala-Zamora, A. I., Forrest, M., and Bechtold, M.: Scenario setup and forcing data for impact model evaluation and impact attribution within the third round of the Inter-Sectoral Impact Model Intercomparison Project (ISIMIP3a), Geoscientific Model Development, 17, 1–51, https://doi.org/10.5194/gmd-17-1-2024, 2024.

Funk, C., Peterson, P., Landsfeld, M., Pedreros, D., Verdin, J., Shukla, S., Husak, G., Rowland, J., Harrison, L., Hoell, A., and Michaelsen, J.: The climate hazards infrared precipitation with stations—a new environmental record for monitoring extremes, Sci Data, 2, 150066, https://doi.org/10.1038/sdata.2015.66, 2015.

Gebrechorkos, S. H., Sheffield, J., Vicente-Serrano, S. M., Funk, C., Miralles, D. G., Peng, J., Dyer, E., Talib, J., Beck, H. E., Singer, M. B., and Dadson, S. J.: Warming accelerates global drought severity, Nature, 1–8, https://doi.org/10.1038/s41586-025-09047-2, 2025.

Guillaume, J. H. A., Helgeson, C., Elsawah, S., Jakeman, A. J., and Kummu, M.: Toward best practice framing of uncertainty in scientific publications: A review of Water Resources Research abstracts, Water Resources Research, 53, 6744–6762, https://doi.org/10.1002/2017WR020609, 2017.

Hanasaki, N., Yoshikawa, S., Pokhrel, Y., and Kanae, S.: A global hydrological simulation to specify the sources of water used by humans, Hydrology and Earth System Sciences, 22, 789–817, https://doi.org/10.5194/hess-22-789-2018, 2018.

Hao, Z., Zhang, X., Pang, Y., Lv, B., and Singh, V. P.: Spatial-temporal monitoring of compound droughts over global land areas, Environmental Modelling & Software, 189, 106463, https://doi.org/10.1016/j.envsoft.2025.106463, 2025.

Howells, M., Hermann, S., Welsch, M., Bazilian, M., Segerström, R., Alfstad, T., Gielen, D., Rogner, H., Fischer, G., van Velthuizen, H., Wiberg, D., Young, C., Roehrl, R. A., Mueller, A., Steduto, P., and Ramma, I.: Integrated analysis of climate change, land-use, energy and water strategies, Nature Clim Change, 3, 621–626, https://doi.org/10.1038/nclimate1789, 2013.

Kallio, M., Heino, M., Kinnunen, P., Fallon, A., and Ahopelto, L.: Identifying Global Co-occurrence of Hydrological, Meteorological and Agricultural Droughts, 2019.

Keune, J., Di Giuseppe, F., Barnard, C., Damasio da Costa, E., and Wetterhall, F.: ERA5–Drought: Global drought indices based on ECMWF reanalysis, Sci Data, 12, 616, https://doi.org/10.1038/s41597-025-04896-y, 2025.

Lavers, D. A., Simmons, A., Vamborg, F., and Rodwell, M. J.: An evaluation of ERA5 precipitation for climate monitoring, Quarterly Journal of the Royal Meteorological Society, 148, 3152–3165, https://doi.org/10.1002/qj.4351, 2022.

Li, L., Peng, Q., Li, Z., and Cai, H.: Evolution of drought characteristics and propagation from meteorological to agricultural drought under the influences of climate change and human activities, Environ Sci Pollut Res, 31, 26713–26736, https://doi.org/10.1007/s11356-024-32709-z, 2024.

Li, T., Song, F., De Cock, A., De Maeyer, P., Bao, J., Yuan, Y., Naibi, S., Bao, A., Ho, L. T., and Goethals, P.: Global disparities in rural and urban population exposure to compound drought and heatwave events, npj Clim Atmos Sci, 8, 1–11, https://doi.org/10.1038/s41612-025-01025-9, 2025.

Li, Y., Lu, H., Yang, K., Wang, W., Tang, Q., Khem, S., Yang, F., and Huang, Y.: Meteorological and hydrological droughts in Mekong River Basin and surrounding areas under climate change, Journal of Hydrology: Regional Studies, 36, 100873, https://doi.org/10.1016/j.ejrh.2021.100873, 2021.

https://doi.org/10.5194/egusphere-2025-3909
Preprint. Discussion started: 3 September 2025

Linke, S., Lehner, B., Ouellet Dallaire, C., Ariwi, J., Grill, G., Anand, M., Beames, P., Burchard-Levine, V., Maxwell, S., Moidu, H., Tan, F., and Thieme, M.: Global hydro-environmental sub-basin and river reach characteristics at high spatial resolution, Sci Data, 6, 283, https://doi.org/10.1038/s41597-019-0300-6, 2019.

Mahecha, M. D., Gans, F., Brandt, G., Christiansen, R., Cornell, S. E., Fomferra, N., Kraemer, G., Peters, J., Bodesheim, P., Camps-Valls, G., Donges, J. F., Dorigo, W., Estupinan-Suarez, L. M., Gutierrez-Velez, V. H., Gutwin, M., Jung, M., Londoño, M. C., Miralles, D. G., Papastefanou, P., and Reichstein, M.: Earth system data cubes unravel global multivariate dynamics, Earth System Dynamics, 11, 201–234, https://doi.org/10.5194/esd-11-201-2020, 2020.

von Matt, C. N., Muelchi, R., Gudmundsson, L., and Martius, O.: Compound droughts under climate change in Switzerland, Natural Hazards and Earth System Sciences, 24, 1975–2001, https://doi.org/10.5194/nhess-24-1975-2024, 2024.

McKee, T. B., Doesken, N. J., and Kleist, J.: THE RELATIONSHIP OF DROUGHT FREQUENCY AND DURATION TO TIME SCALES, Eighth Conference on Applied Climatology, Anaheim, California, 1993.

Meybeck, M., Kummu, M., and Dürr, H. H.: Global hydrobelts and hydroregions: improved reporting scale for water-related issues?, Hydrology and Earth System Sciences, 17, 1093–1111, https://doi.org/10.5194/hess-17-1093-2013, 2013.

Mishra, A. K. and Singh, V. P.: A review of drought concepts, Journal of Hydrology, 391, 202–216, https://doi.org/10.1016/j.jhydrol.2010.07.012, 2010.

Mo, K. C. and Lettenmaier, D. P.: Objective Drought Classification Using Multiple Land Surface Models, Journal of Hydrometeorology, 15, 990–1010, https://doi.org/10.1175/JHM-D-13-071.1, 2014.

Mukherjee, S., Mishra, A., and Trenberth, K. E.: Climate Change and Drought: a Perspective on Drought Indices, Curr Clim Change Rep, 4, 145–163, https://doi.org/10.1007/s40641-018-0098-x, 2018.

Müller Schmied, H., Trautmann, T., Ackermann, S., Cáceres, D., Flörke, M., Gerdener, H., Kynast, E., Peiris, T. A., Schiebener, L., Schumacher, M., and Döll, P.: The global water resources and use model WaterGAP v2.2e: description and evaluation of modifications and new features, Geoscientific Model Development Discussions, 1–46, https://doi.org/10.5194/gmd-2023-213, 2023.

NOAA (National Oceanic and Atmospheric Administration): Niño 3.4 SST Index from the NOAA ERSST V5, 2025.

Porkka, M., Virkki, V., Wang-Erlandsson, L., Gerten, D., Gleeson, T., Mohan, C., Fetzer, I., Jaramillo, F., Staal, A., te Wierik, S., Tobian, A., van der Ent, R., Döll, P., Flörke, M., Gosling, S. N., Hanasaki, N., Satoh, Y., Müller Schmied, H., Wanders, N., Famiglietti, J. S., Rockström, J., and Kummu, M.: Notable shifts beyond pre-industrial streamflow and soil moisture conditions transgress the planetary boundary for freshwater change, Nat Water, 2, 262–273, https://doi.org/10.1038/s44221-024-00208-7, 2024.

Quichimbo, E. A., Singer, M. B., Michaelides, K., Hobley, D. E. J., Rosolem, R., and Cuthbert, M. O.: DRYP 1.0: a parsimonious hydrological model of DRYland Partitioning of the water balance, Geoscientific Model Development, 14, 6893–6917, https://doi.org/10.5194/gmd-14-6893-2021, 2021.

Reinecke, R., Stein, L., Gnann, S., Andersson, J. C. M., Arheimer, B., Bierkens, M., Bonetti, S., Güntner, A., Kollet, S., Mishra, S., Moosdorf, N., Nazari, S., Pokhrel, Y., Prudhomme, C., Schewe, J., Shen, C., and Wagener, T.: Uncertainties as a Guide for Global Water Model Advancement, WIREs Water, 12, e70025, https://doi.org/10.1002/wat2.70025, 2025.

Rivoire, P., Martius, O., and Naveau, P.: A Comparison of Moderate and Extreme ERA-5 Daily Precipitation With Two Observational Data Sets, Earth and Space Science, 8, e2020EA001633, https://doi.org/10.1029/2020EA001633, 2021.

https://doi.org/10.5194/egusphere-2025-3909
Preprint. Discussion started: 3 September 2025

Sarhadi, A., Modarres, R., and Vicente-Serrano, S. M.: Dynamic compound droughts in the Contiguous United States, Journal of Hydrology, 626, 130129, https://doi.org/10.1016/j.jhydrol.2023.130129, 2023.

Sen, P. K.: Estimates of the Regression Coefficient Based on Kendall's Tau, Journal of the American Statistical Association, 63, 1379–1389, https://doi.org/10.1080/01621459.1968.10480934, 1968.

Shakeel, M., Abbas, H., Waseem, A., and Ali, Z.: Adaptive ensemble weighting for GCMs to enhance future drought characterization under various climate change scenarios, Theor Appl Climatol, 156, 269, https://doi.org/10.1007/s00704-025-05516-w, 2025.

Singh, J., Ashfaq, M., Skinner, C. B., Anderson, W. B., and Singh, D.: Amplified risk of spatially compounding droughts during co-occurrences of modes of natural ocean variability, npj Clim Atmos Sci, 4, 7, https://doi.org/10.1038/s41612-021-00161-2, 2021.

Singh, J., Ashfaq, M., Skinner, C. B., Anderson, W. B., Mishra, V., and Singh, D.: Enhanced risk of concurrent regional droughts with increased ENSO variability and warming, Nat. Clim. Chang., 12, 163–170, https://doi.org/10.1038/s41558-021-01276-3, 2022.

Spinoni, J., Barbosa, P., Bucchignani, E., Cassano, J., Cavazos, T., Christensen, J. H., Christensen, O. B., Coppola, E., Evans, J., Geyer, B., Giorgi, F., Hadjinicolaou, P., Jacob, D., Katzfey, J., Koenigk, T., Laprise, R., Lennard, C. J., Kurnaz, M. L., Li, D., Llopart, M., McCormick, N., Naumann, G., Nikulin, G., Ozturk, T., Panitz, H.-J., Rocha, R. P. da, Rockel, B., Solman, S. A., Syktus, J., Tangang, F., Teichmann, C., Vautard, R., Vogt, J. V., Winger, K., Zittis, G., and Dosio, A.: Future Global Meteorological Drought Hot Spots: A Study Based on CORDEX Data, https://doi.org/10.1175/JCLI-D-19-0084.1, 2020.

Tiwari, A. D., Pokhrel, Y., Boulange, J., Burek, P., Guillaumot, L., Gosling, S. N., Grillakis, M., Hanasaki, N., Koutroulis, A., Ostberg, S., Otta, K., Schmied, H. M., Satoh, Y., Scanlon, B., Stacke, T., and Yokohata, T.: Similarities and divergent patterns in hydrologic fluxes and storages simulated by global water models, Nat Water, 3, 550–560, https://doi.org/10.1038/s44221-025-00435-6, 2025.

Van Loon, A. F.: Hydrological drought explained, WIREs Water, 2, 359–392, https://doi.org/10.1002/wat2.1085, 2015.

Vicente-Serrano, S. M., Beguería, S., and López-Moreno, J. I.: A Multiscalar Drought Index Sensitive to Global Warming: The Standardized Precipitation Evapotranspiration Index, Journal of Climate, 23, 1696–1718, https://doi.org/10.1175/2009JCLI2909.1, 2010.

Vieira, M. J. F. and Stadnyk, T. A.: Leveraging global climate models to assess multi-year hydrologic drought, npj Clim Atmos Sci, 6, 1–12, https://doi.org/10.1038/s41612-023-00496-y, 2023.

van Vliet, M. T. H., Wiberg, D., Leduc, S., and Riahi, K.: Power-generation system vulnerability and adaptation to changes in climate and water resources, Nature Clim Change, 6, 375–380, https://doi.org/10.1038/nclimate2903, 2016.

Walker, W. E., Haasnoot, M., and Kwakkel, J. H.: Adapt or Perish: A Review of Planning Approaches for Adaptation under Deep Uncertainty, Sustainability, 5, 955–979, https://doi.org/10.3390/su5030955, 2013.

Wang, T., Tu, X., Singh, V. P., Chen, X., and Lin, K.: Global data assessment and analysis of drought characteristics based on CMIP6, Journal of Hydrology, 596, 126091, https://doi.org/10.1016/j.jhydrol.2021.126091, 2021.

Wilhite, D. and Glantz, M.: Understanding: the Drought Phenomenon: The Role of Definitions, Water International, 10, 111–120, https://doi.org/10.1080/02508068508686328, 1985.

https://doi.org/10.5194/egusphere-2025-3909
Preprint. Discussion started: 3 September 2025

Wu, J., Yao, H., Chen, X., Wang, G., Bai, X., and Zhang, D.: A framework for assessing compound drought events from a drought propagation perspective, Journal of Hydrology, 604, 127228, https://doi.org/10.1016/j.jhydrol.2021.127228, 2022.

Yang, G., Chang, J., Wang, Y., Guo, A., Zhang, L., Zhou, K., and Wang, Z.: Understanding drought propagation through coupling spatiotemporal features using vine copulas: A compound drought perspective, Science of The Total Environment, 921, 171080, https://doi.org/10.1016/j.scitotenv.2024.171080, 2024.

Yejyevich, V.: AN OBJECTIVE APPROACH TO DEFINITIONS AND INVESTIGATIONS OF CONTINENTAL HYDROLOGIC DROUGHTS, Colorado State University, Fort Collins, Colorado, 1967.

Yokohata, T., Kinoshita, T., Sakurai, G., Pokhrel, Y., Ito, A., Okada, M., Satoh, Y., Kato, E., Nitta, T., Fujimori, S., Felfelani, F., Masaki, Y., Iizumi, T., Nishimori, M., Hanasaki, N., Takahashi, K., Yamagata, Y., and Emori, S.: MIROC-INTEG-LAND version 1: a global biogeochemical land surface model with human water management, crop growth, and land-use change, Geoscientific Model Development, 13, 4713–4747, https://doi.org/10.5194/gmd-13-4713-2020, 2020.

Zhang, X., Hao, Z., Singh, V. P., Zhang, Y., Feng, S., Xu, Y., and Hao, F.: Drought propagation under global warming: Characteristics, approaches, processes, and controlling factors, Science of The Total Environment, 838, 156021, https://doi.org/10.1016/j.scitotenv.2022.156021, 2022.

Zscheischler, J., Martius, O., Westra, S., Bevacqua, E., Raymond, C., Horton, R. M., van den Hurk, B., AghaKouchak, A., Jézéquel, A., Mahecha, M. D., Maraun, D., Ramos, A. M., Ridder, N. N., Thiery, W., and Vignotto, E.: A typology of compound weather and climate events, Nature Reviews Earth & Environment, 1, 333–347, https://doi.org/10.1038/s43017-020-0060-z, 2020.